Science with ALMA

- Key science goal includes
  - Image protoplanetary disks to detect tidal gaps created by planets undergoing formation in the disks;
  - Image normal galaxies like the Milky Way (in CO or CII line, for example) out to Z=3
  - Precision imaging at high angular resolution(0.1")

- General Science Requirements, from ALMA Project Plan v2.0: "ALMA should provide astronomers with a general purpose telescope which they can use to study at a range of angular resolutions millimeter and submillimeter wavelength emission from all kinds of astronomical sources. ALMA will be an appropriate successor to the present generation of millimeter wave interferometric arrays and will allow astronomers to:
  - Image the redshifted dust continuum emission from evolving galaxies at epochs of formation as early as z=10;
  - Trace through molecular and atomic spectroscopic observations the chemical composition of star-forming gas in galaxies throughout the history of the Universe;
  - Reveal the kinematics of obscured galactic nuclei and Quasi-Stellar Objects on spatial scales smaller than 300 light years;
  - Image gas rich, heavily obscured regions that are spawning protostars, protoplanets and pre-planetary disks;
  - Reveal the crucial isotopic and chemical gradients within circumstellar shells that reflect the chronology of invisible stellar nuclear processing;
  - Obtain unobscured, sub-arcsecond images of cometary nuclei, hundreds of asteroids, Centaurs, and Kuiper Belt Objects in the solar system along with images of the planets and their satellites;
  - Image solar active regions and investigate the physics of particle acceleration on the surface of the sun.

Recent ALMA Publications (data from Science Verification and Cycle 0)

Over 600 entries from the ADS search with keyword "ALMA" in the Abstract from 2011 to now

Recent ALMA Publications (data from Science Verification and Cycle 0)

ALMA CO and VLT/SINFONI H_2 observations of the Antennae overlap region: mass and energy dissipation, Herrera et al. 2012, A&A

- Evidence for Multiple Pathways to Deuterium Enhancements in Protoplanetary Disks, Oberg et al. 2012, ApJ
- ALMA's View of Molecular Gas in 30 Doradus, Indebetouw et al. 2012, AAS
- Probing the Molecular Outflows of the Coldest Known Object in the Universe: The Boomerang Nebula, Sahai et al. 2012, AAS
- Constraining the Planetary System of Fomalhaut Using High-resolution ALMA Observations, Boley et al. 2012, ApJ
- ALMA reveals a chemically evolved submillimeter galaxy at z = 4.76, Nagao et al. 2012, A&A
- [C II] Line Emission in Massive Star-forming Galaxies at z = 4.7, Wagg et al. 2012, ApJ
- ALMA Observations of the Outflow from Source I in the Orion-KL Region, Zapata et al. 2012, ApJ
- The first ALMA view of IRAS 16293-2422. Direct detection of infall onto source B and high-resolution kinematics of source A, Pineda et al. 2012, A&A
- The First Detection of the 232 GHz Vibrationally Excited H_2O Maser in Orion KL with ALMA, Hirota et al. 2012, ApJ
- Detection of the Simplest Sugar, Glycolaldehyde, in a Solar-type Protostar with ALMA, Jorgensen et al. 2012, ApJ
- ALMA Submillimeter Continuum Imaging of the Host Galaxies of GRB 021004 and GRB 080607, Wang et al. 2012, ApJL
- An ALMA survey of submillimetre galaxies in the Extended Chandra Deep Field South: High resolution 870um source counts, Karim et al. 2012, arXiv
- An ALMA survey of submillimetre galaxies in the Extended Chandra Deep Field-South: detection of [C II] at z = 4.4, Swinbank et al. 2012, MNRAS

Recent ALMA Publications (data from Science Verification and Cycle 0)

- Kinematics of the CO Gas in the Inner Regions of the TW Hya Disk, Rosenfeld et al. 2012, ApJ
- Unexpectedly large mass loss during the thermal pulse cycle of the red giant star R Sculptoris, M. Maercker et al. 2012, Nature
- ALMA and VLA observations of recombination lines and continuum toward the Becklin-Neugebauer object in Orion, Galvan-Madrid et al. 2012, A&A
- Outflow Structure and Velocity Field of Orion Source I: ALMA Imaging of SiO Isotopologue Maser and Thermal Emission, Niederhofer et al. 2012, A&A
- ALMA Observations of ρ-Oph 102: Grain Growth and Molecular Gas in the Disk around a Young Brown Dwarf, Ricci et al. 2012, ApJL
- ALMA and VLA observations of the outflows in IRAS 16293-2422, Loinard et al. 2012, MNRAS
- Warm water deuterium fractionation in IRAS 16293-2422. The high-resolution ALMA and SMA view, Persson et al. 2013, A&A
- ALMA CO J = 6-5 observations of IRAS 16293-2422. Shocks and entrainment, Kristensen et al. 2013, A&A
- ALMA Observations of Transitional Disks, Perez et al. 2013, AAS
- ALMA Observations of the Brightest Starbursts in the Universe, Marrone et al. 2013, AAS
- [C II] Line Emission and Star Formation from Quasar Host Galaxies at 6, Wang et al. 2013, AAS
- Millimeter Emission Structure in the First ALMA Image of the AU Mic Debris Disk, MacGregor et al. 2013, ApJ
- ALMA 690 GHz observations of IRAS 16293-2422B: Infall in a highly optically-thick disk, Zapata et al. 2013, arXiv

ALMA CO and VLT/SINFONI H2 observations of the Antennae overlap region: mass and energy dissipation

C. N. Herrera1, F. Boulanger, N. P. H. Nesvadba, and E. Falgarone

2012, A&A, 538, L9

Science Verification Data

Antennae Galaxies composite of ALMA and Hubble observations

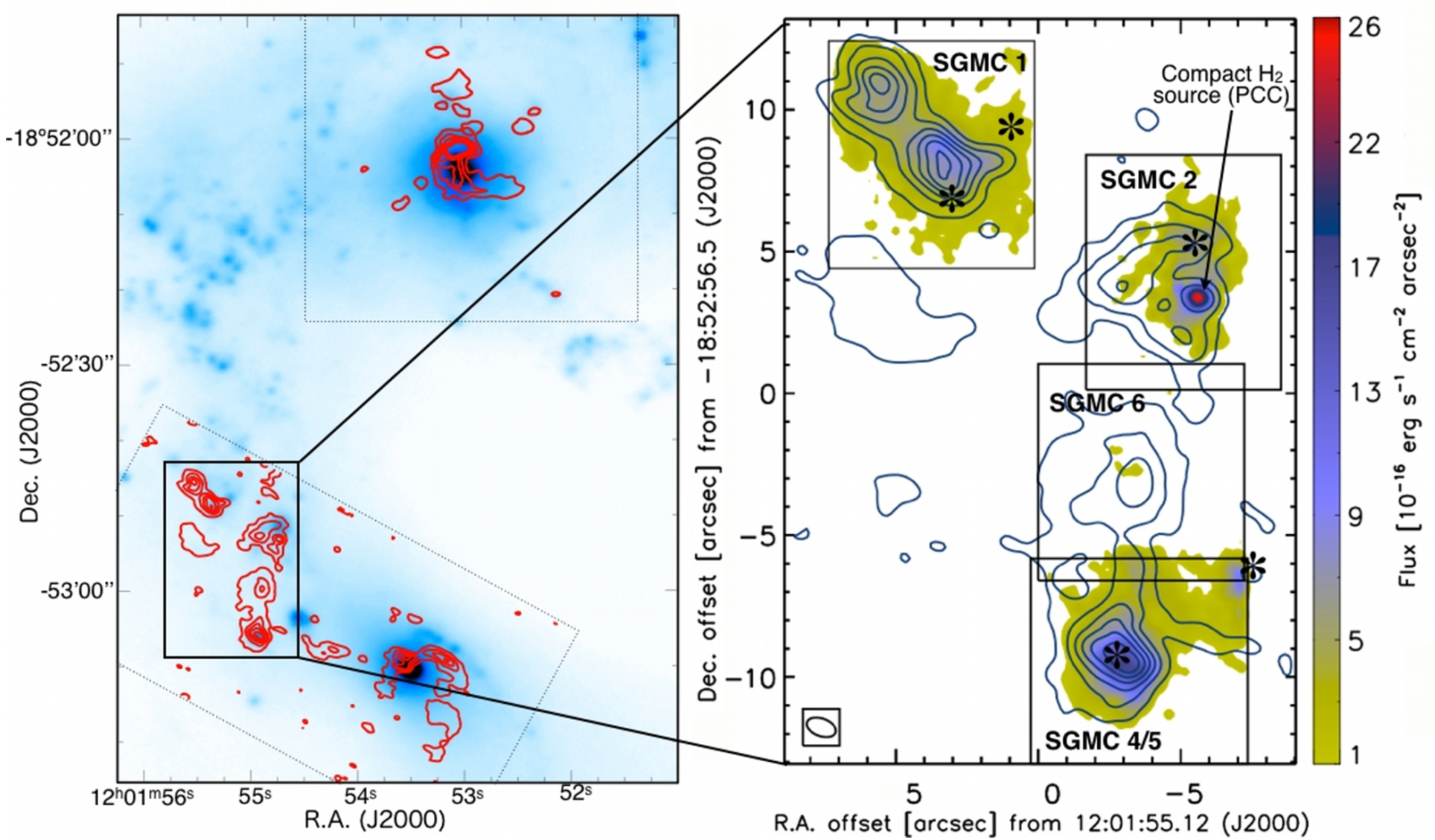

Figure 1:

Left. ALMA CO morphology shown on top of our CFHT *K*-band continuum image (Herrera et al, 2011). Dotted boxes mark the two ALMA mosaics, the solid box marks the overlap region. *Right.* H_2 1−0 S(1) morphology as seen with SINFONI. Boxes mark individual SINFONI fields-of-view, contours show CO(3−2) from 2 to 42 Jy km s^{-1} $beam^{-1}$ in steps of 8 Jy km s^{-1} $beam^{-1}$. The inset at the bottom left of the right panel shows the ALMA beam. We also mark massive and young super star clusters (SSCs) (asterisks), and the compact H_2 source pre cluster cloud (PCC).

Wilson et al. (2000)

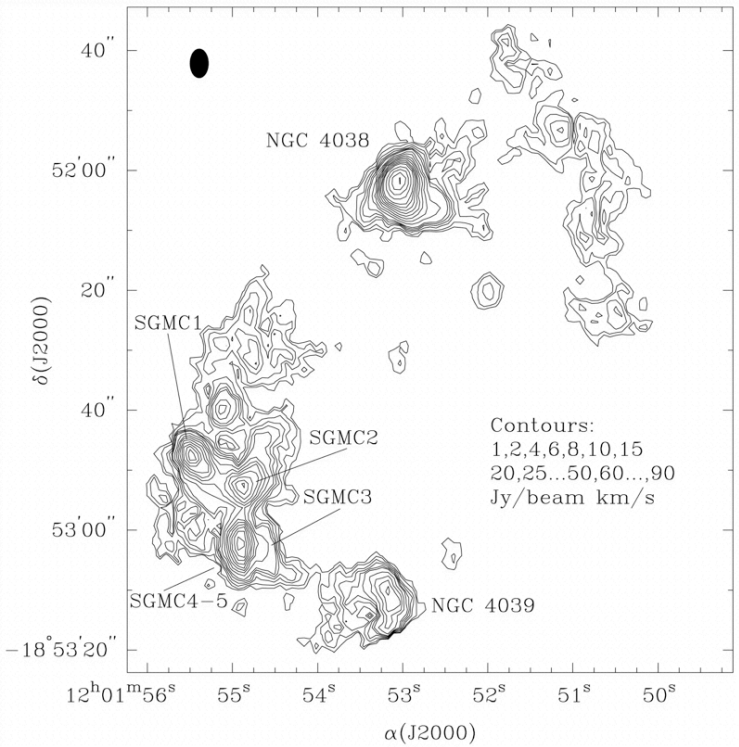

Ueda et al. (2012)

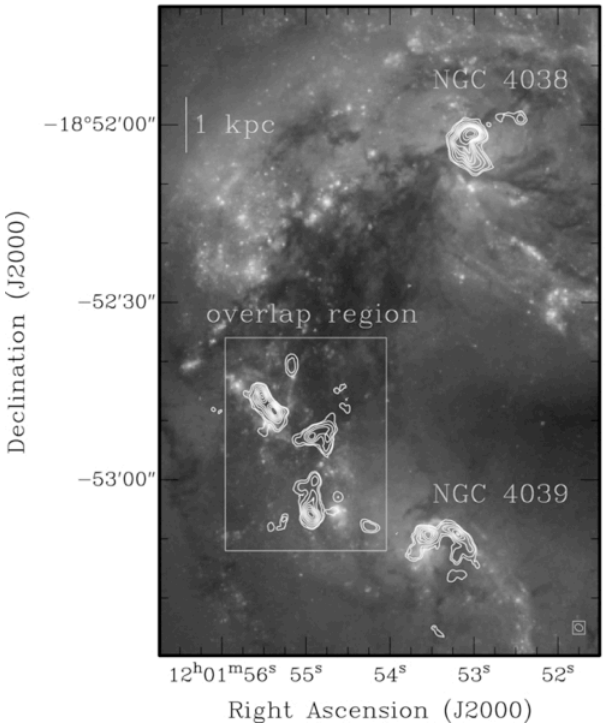

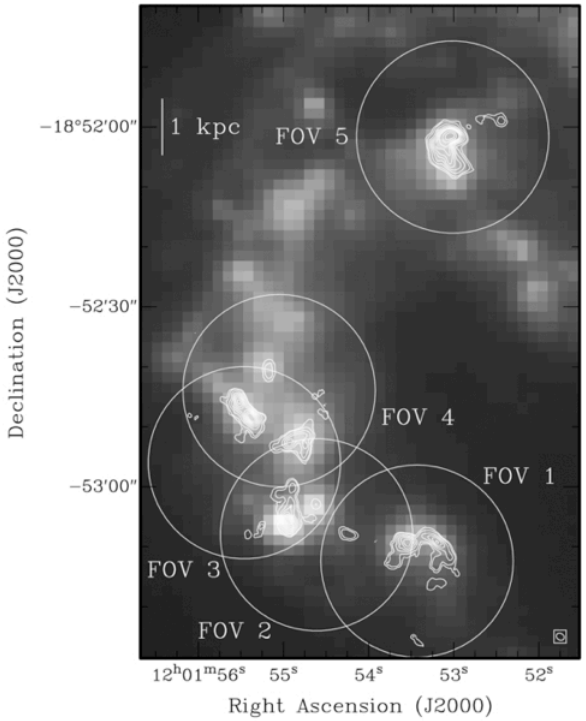

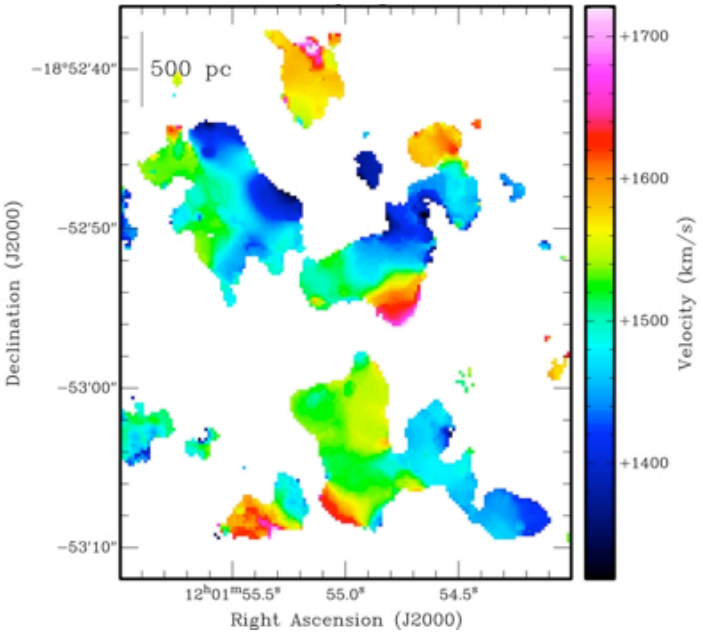

Ueda et al. (2012)

EVIDENCE FOR MULTIPLE PATHWAYS TO DEUTERIUM ENHANCEMENTS IN PROTOPLANETARY DISKS

Karin I. Oberg, Chunhua Qi, David J. Wilner, and Michiel R. Hogerheijde

2012, ApJ, 749 162

Science Verification Data

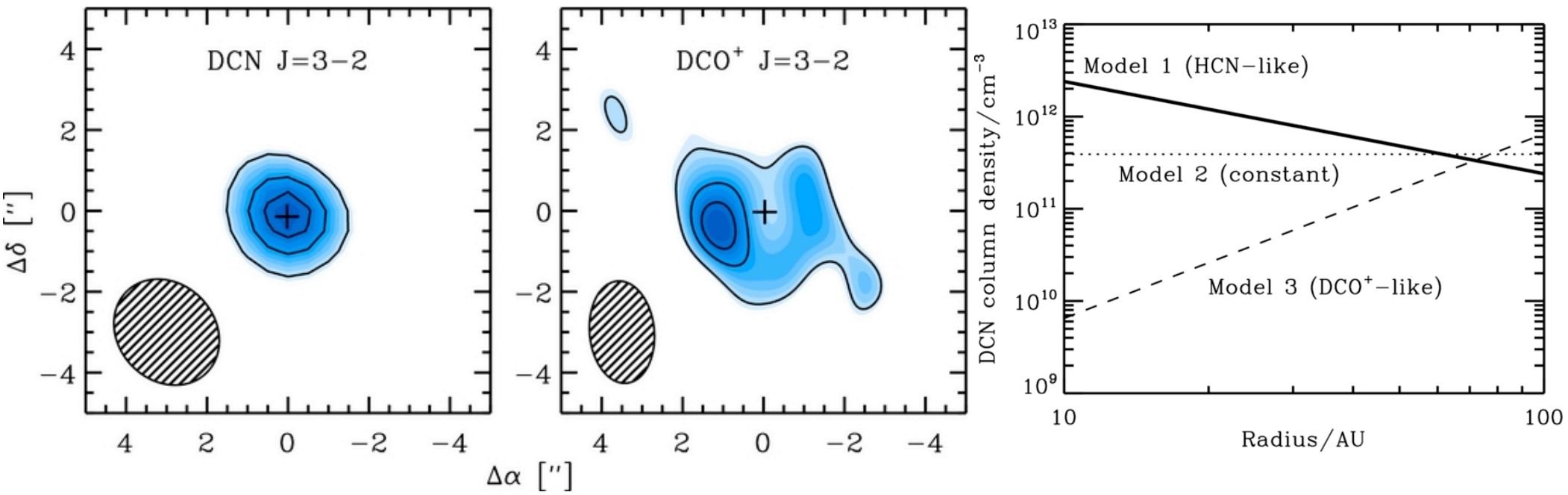

Left (Figure1) : Integrated images of the TW Hya disk in (left) DCN J = 3-2 emission (ALMA science verification) and (right) DCO^+ J = 3-2 emission (SMA data from Qi et al. 2008). The contour levels are at 50%, 75%, and 90% of the peak value. The cross marks the peak of the continuum emission, which locates the position of the central star.

Right (Figure 2): Best-fit radial column density distributions of DCN in the disk around TW Hya from 10 to 100 AU for a falling power law ($\alpha = -2$, thick line), a rising power law ($\alpha = 2$, dashed line), and a constant ($\alpha = 0$, dotted line).

- The observations demonstrate that DCN is centrally peaked on the size scales observed, ruling out common radial distributions for DCN and DCO+. The presence of DCN closer to the star, in regions that are warmer due to stellar irradiation, together with the comparable estimates for the DCN/HCN and DCO+/HCO+ abundance ratios, suggests a mechanism for efficient deuterium enhancement in disk material at higher temperatures than implied by reactions solely with H2D+ at T < 30 K. This agrees with standard model predictions in that DCN can form from gas-phase reactions involving CH2D+ at T > 30 K.
- Other possible mechanisms for the different DCN/DCO+ distribution are discussed but ruled out
  - dynamical transport of cold chemistry products to warmer disk regions
  - photochemistry
  - additional gas-phase reactions that result in HCN deuterium fractionation
  - grain surface formation of DCN followed by desorption
  - molecule-specific destruction such as depletion onto interstellar grains.
- The substantial deuterium enhancement in warmer regions of the TW Hya disk challenges the conventional wisdom that the high deuterium fractions in comets are necessary evidence for a cold (T < 30 K) chemical history (Mumma & Charnley 2011).

Constraining the Planetary System of Fomalhaut Using High-Resolution ALMA Observations

A. C. Boley, M. J. Payne, S. Corder, W. Dent, E. B. Ford, and M. Shabram

Cycle 0 Data

ALMA Reveals Workings of Nearby Planetary System

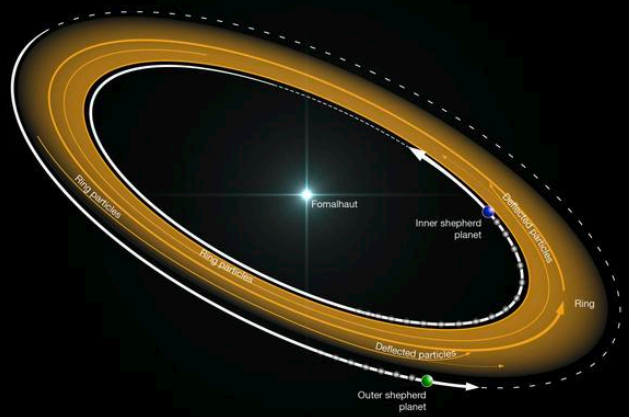

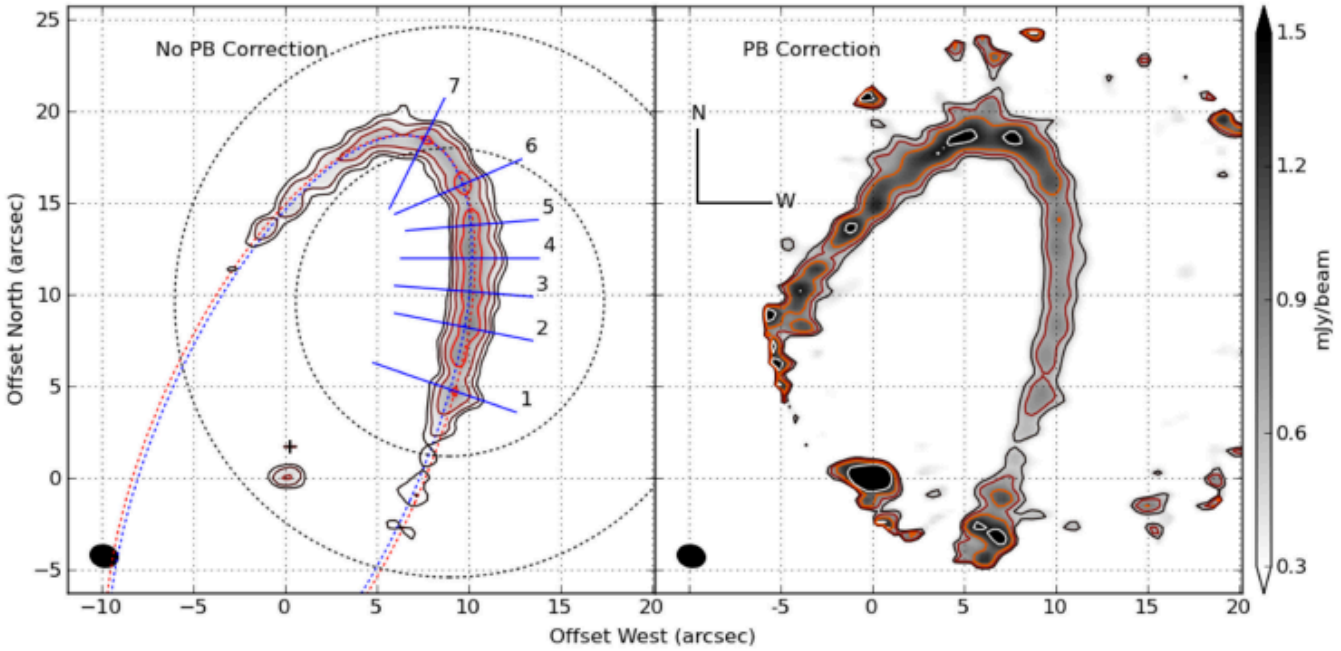

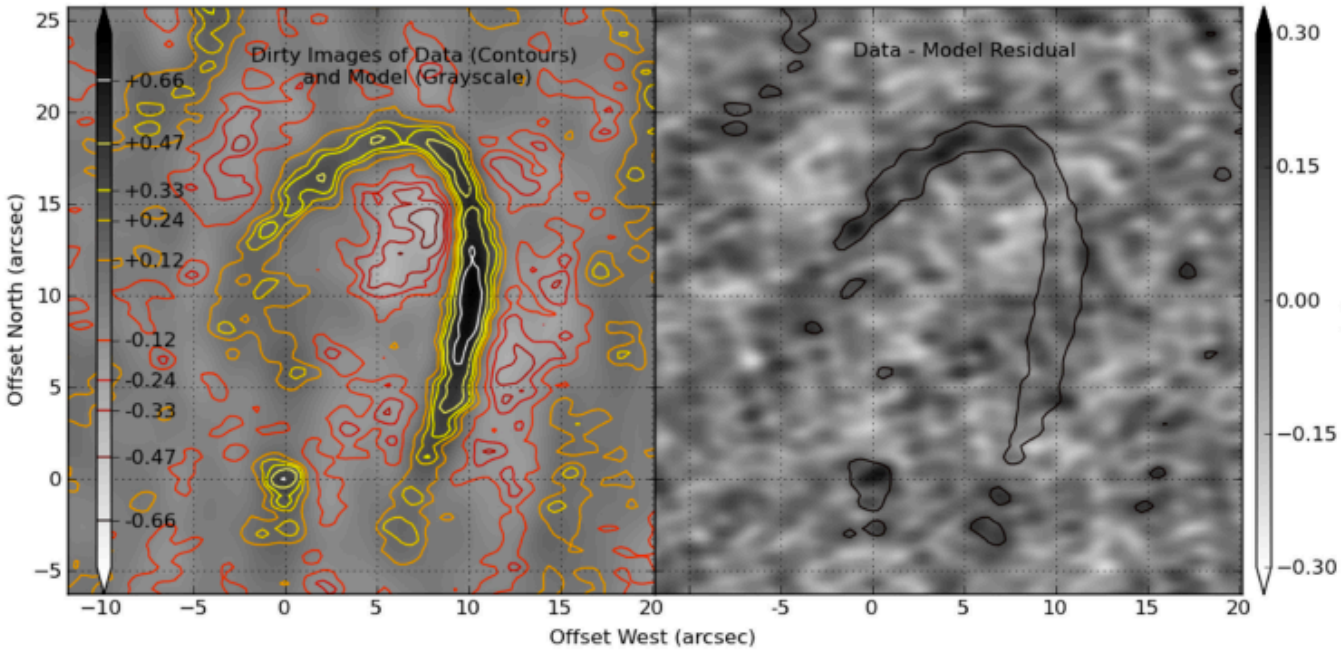

Top-left: 350 GHz ALMA image of Fomalhaut's ring. The RMS noise is 60 Jy beam^{-1}, and the contours represent 0.24, 0.33, 0.47, 0.66, 0.92, and 1.4 mJy beam^{-1}. The circles are centered on the pointing center, and their diameters show the beam's half and 7% power. Ellipses with PA = 336, and i = 66 (red) and 67 (blue) are shown, with the ellipse centers given by the plus sign. The slices labeled 1-7 are used to show surface brightness profiles in Figure 2. The coordinate axis is centered on the star, which has a peak brightness of 0:49 mJy beam^{-1} (uncorrected).

Top-right: The primary beam corrected image. The ring becomes bright near the ansa, and remains bright through the inferred apocenter. The contours are the same as in the top-left, but begin at 0.47 mJy beam^{-1}.

Bottom-left: The best-fit skymodel is compared with the dirty ALMA image. The grayscale and contours show mJy beam^{-1}, with the contour levels labeled on the colorbar.

Bottom-right: The residual of the data minus the model. The model subtracts the emission well, but there remains excess emission in the NE and around the star.

ALMA (B6) Science Verification data on OrionKL

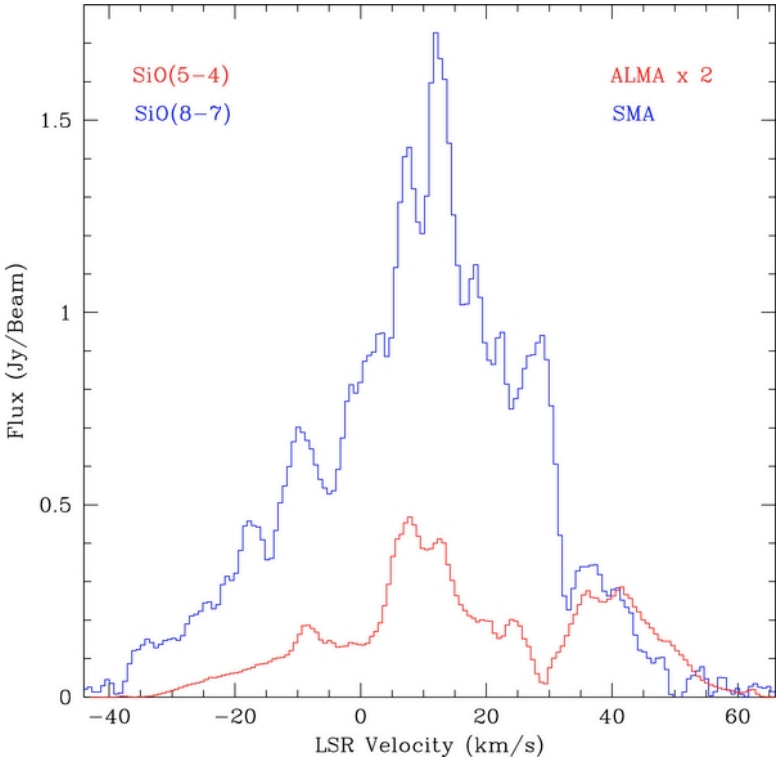

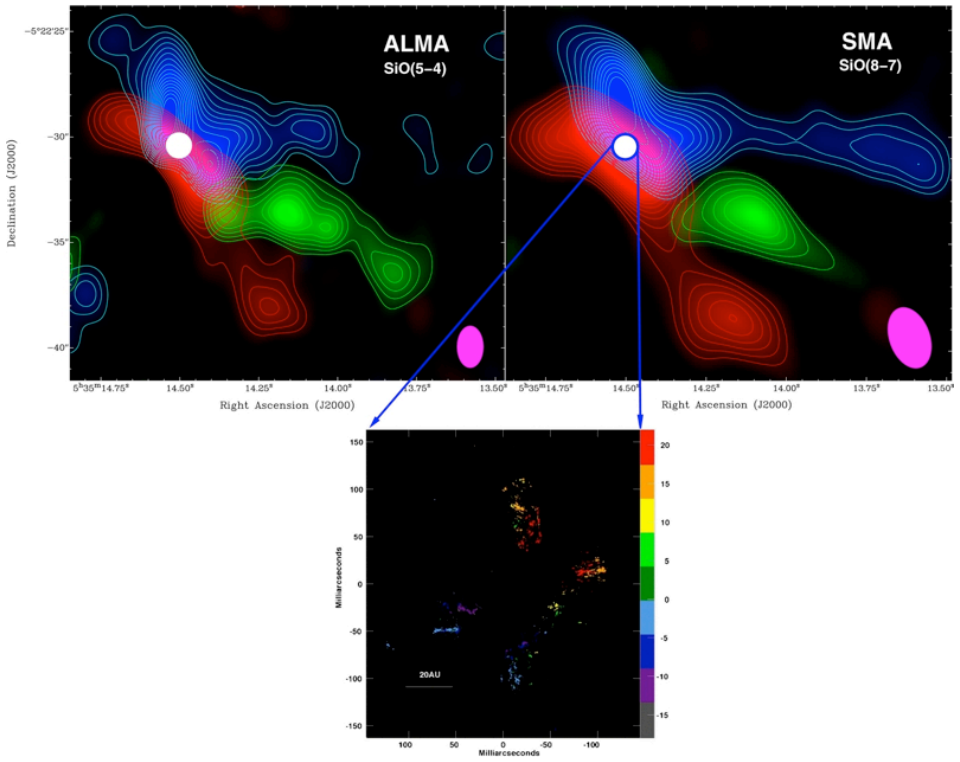

- at scales of a few thousand AU, the outflow has a marked "butterfly" morphology along a northeast-southwest axis. at scales of tens of AU found in the SiO and H_2O maser observations, the blueshifted radial velocities of the moving gas are found to the northwest, while the redshifted velocities are in the southeast.

- possible scenarios include *) two biploar outflows, *) ballistic ejecta from a rotating disk, and *) a single expanding wide-angle northest-southwest, but all inconclusive

(Zapata et al. 2012, ApJ)

ALMA (B6) Science Verification data on OrionKL

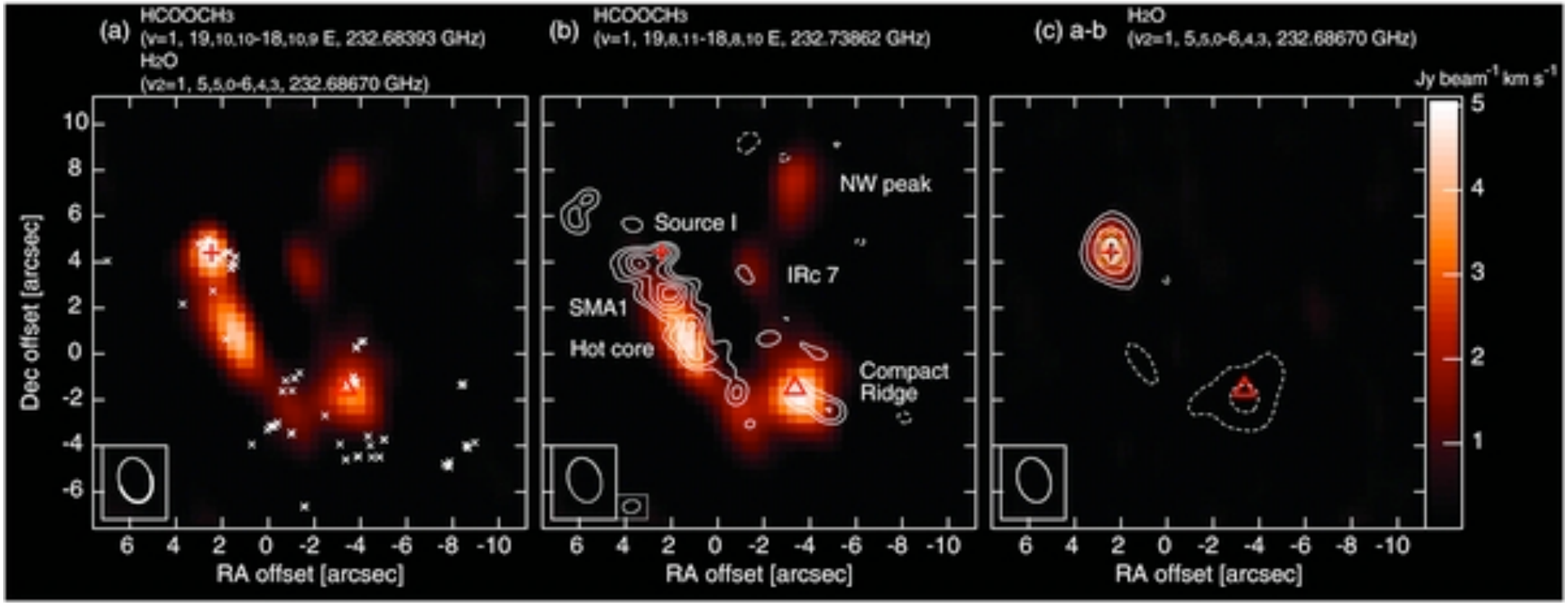

- this is the first detection of the 232 GHz vibrationally excited H_2O maser in star-forming regions.
- The distribution of the 232 GHz maser is concentrated at the position of the radio Source I.

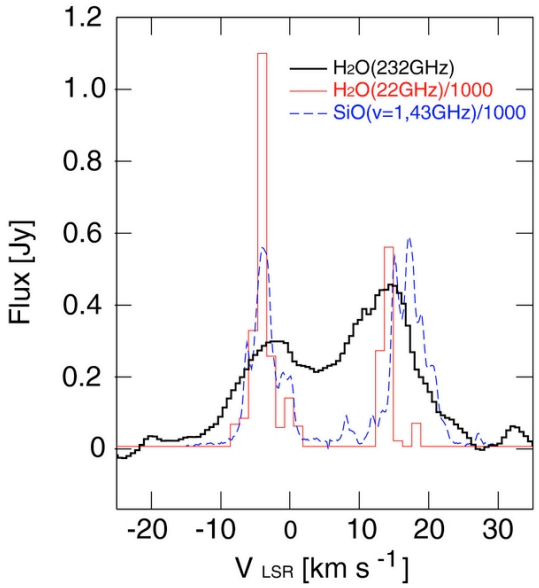

(Hirota et al. 2012, ApJ)

ALMA (B6) Science Verification data on IRAS 16293-2422

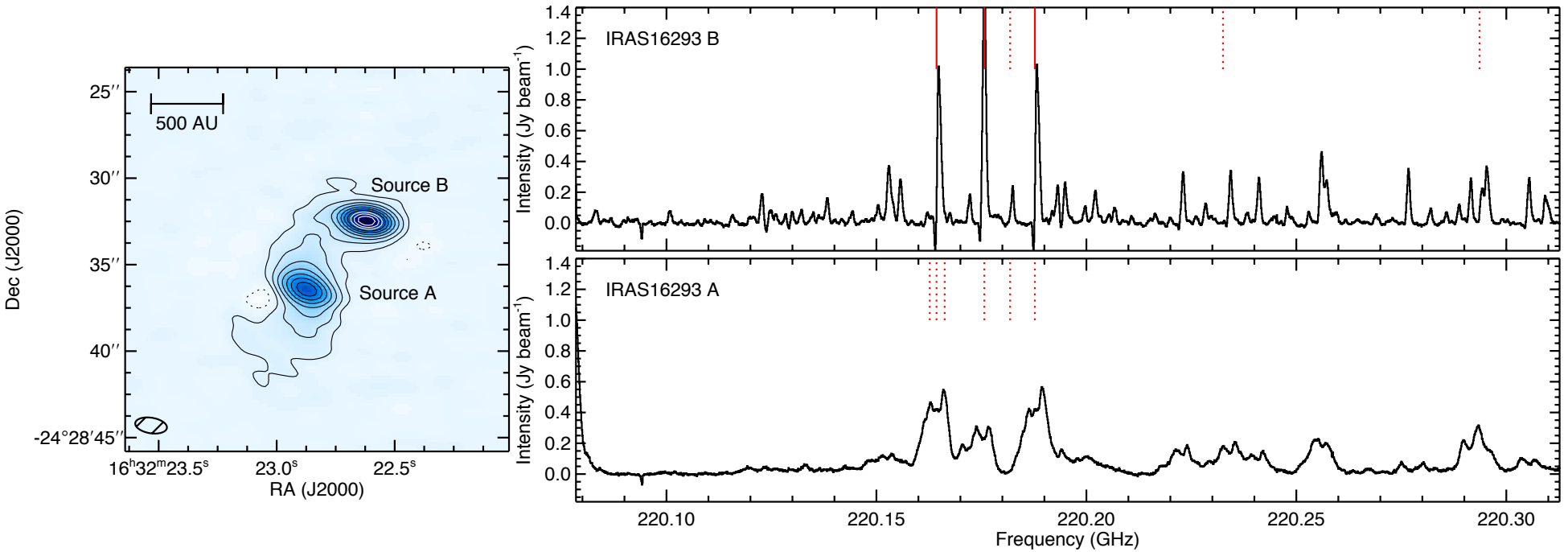

- an inverse P-Cygni profile toward source B in the three brightest lines.
- The line profiles are fitted with a simple two-layer model to derive an infall rate of 4.5×10^{-5} $M_\odot$ yr^{-1}.

(Pineda et al. 2012, A&A)

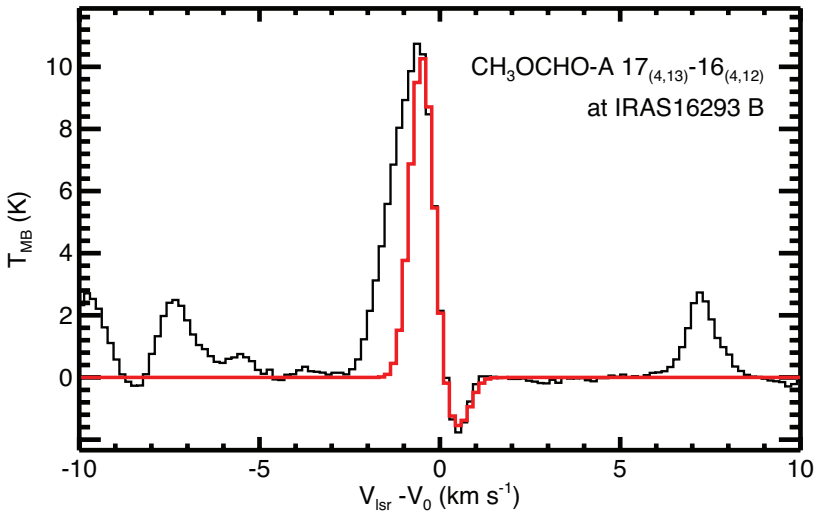

ALMA (B9) Science Verification data on IRAS 16293-2422

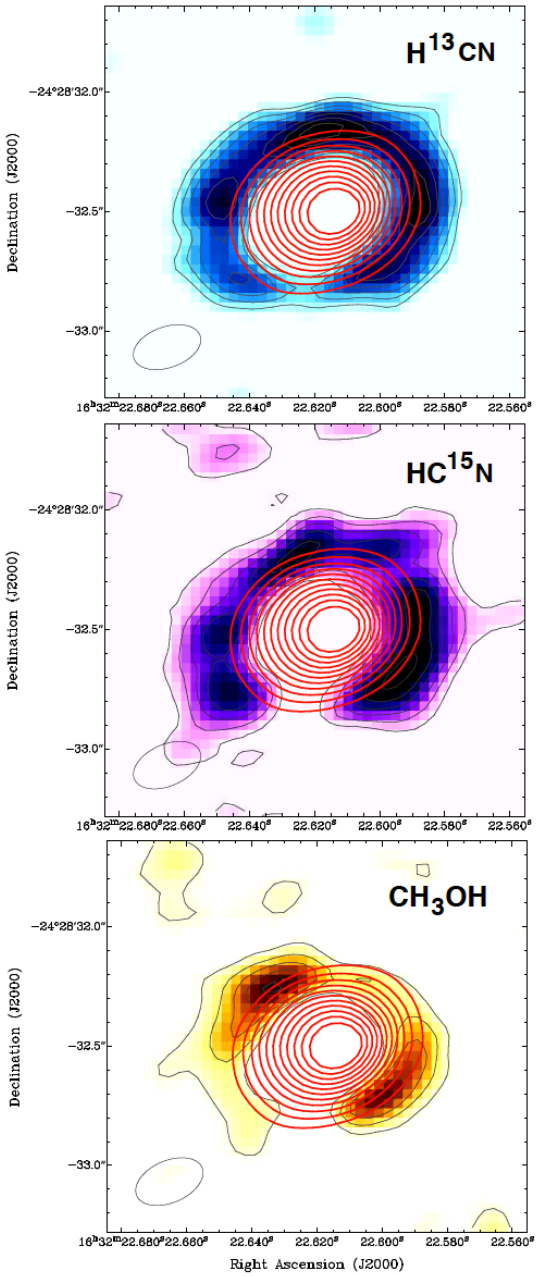

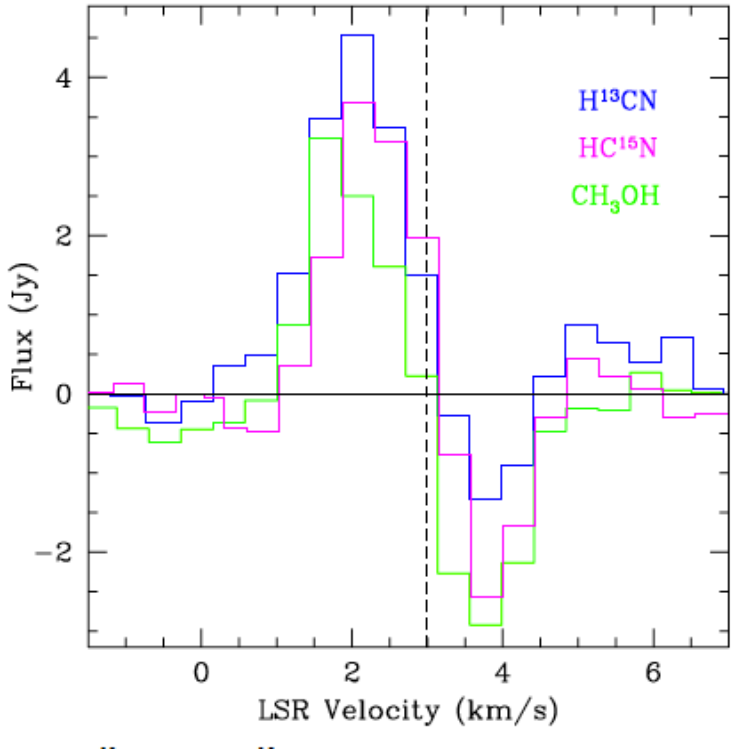

- The 0.45 mm continuum emission revealed a very compact object with a deconvolved angular size of about 400milli-arcseconds that is associated with IRAS 16293-2422B.
- All three lines also show inverse P-Cygni profiles with infall and dispersion velocities larger than those recently reported at smaller wavelengths, suggesting that we are revealing faster, and more turbulent gas located closer to the central object.

(Zapata et al. 2013, arXiv)

Detection of the Simplest Sugar, Glycolaldehyde, in a Solar-type Protostar with ALMA

The Astrophysical Journal Letters, Volume 757, Issue 1

Jes K Jørgensen, Cécile Favre, Suzanne E Bisschop et al.

Reported by Tiara Hung @ RAL group meeting on Jan, 8th

Sweet Result from ALMA

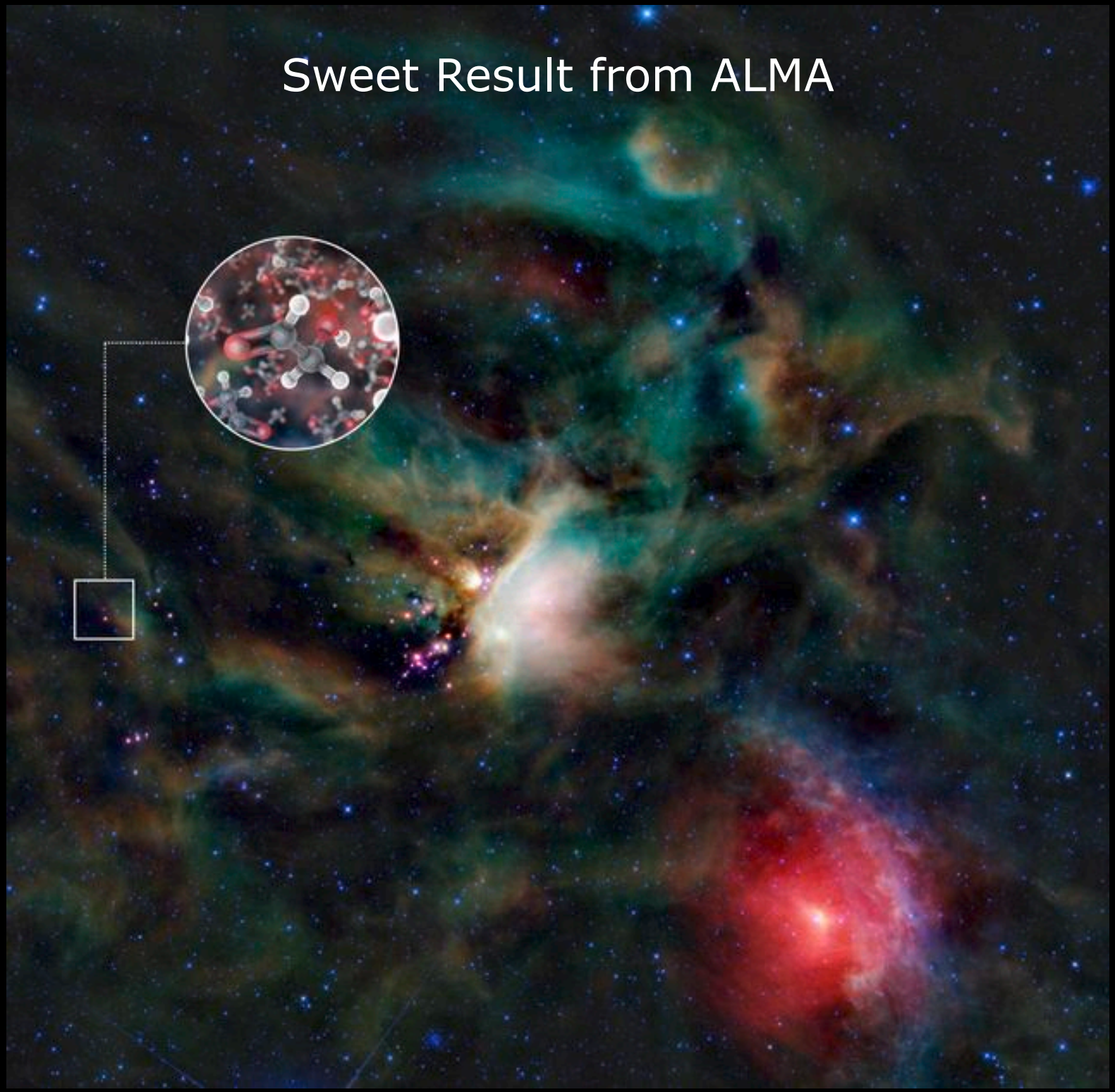

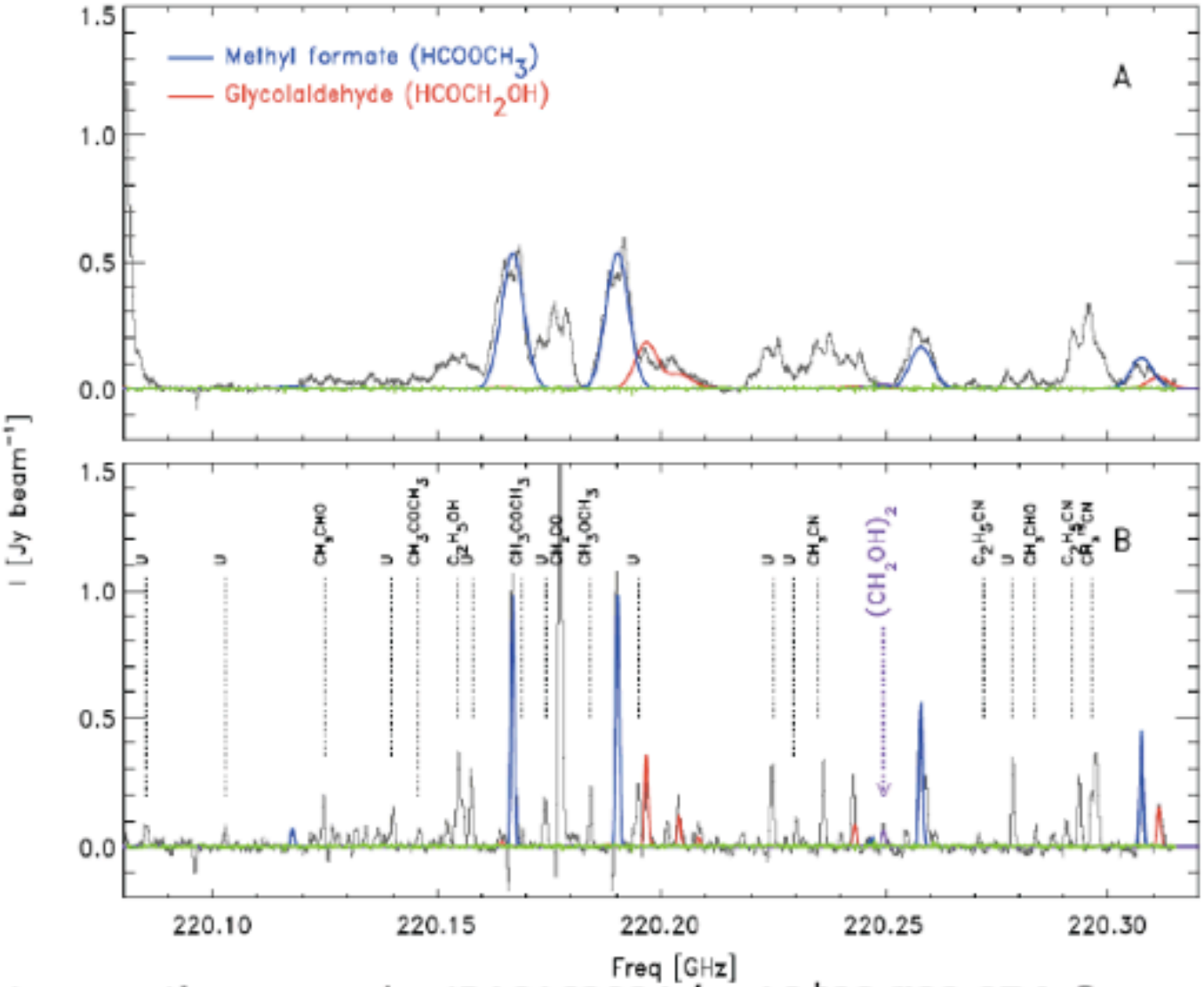

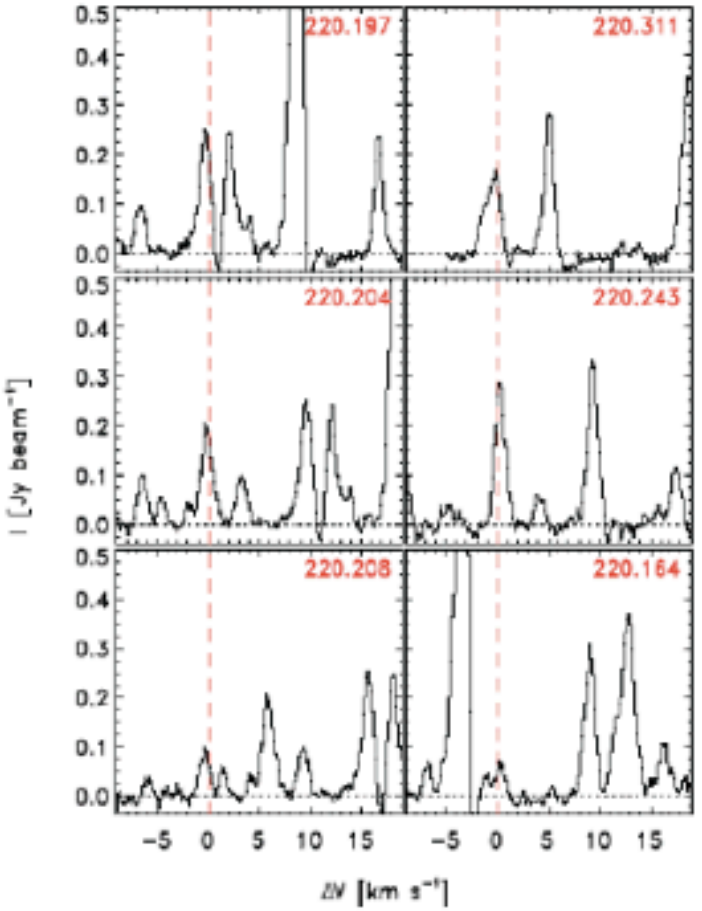

two continuum peaks: IRAS16293A (α=16.^{h}32.^{m}22.87.^{s}; δ= −24.^{d}28′36.″39) and IRAS16293B (α=16.^{h}32.^{m}22.62.^{s}; δ= −24.^{d}28′32.″46). Fits from LTE models of the methyl formate (blue) and glycolaldehyde (red) emission are overplotted.

Wang et al. 2012

ALMA 345 GHz Continuum Imaging

Constraining IR Luminosity and SFR of GRB Host Galaxies

z ~ 2 z ~ 3

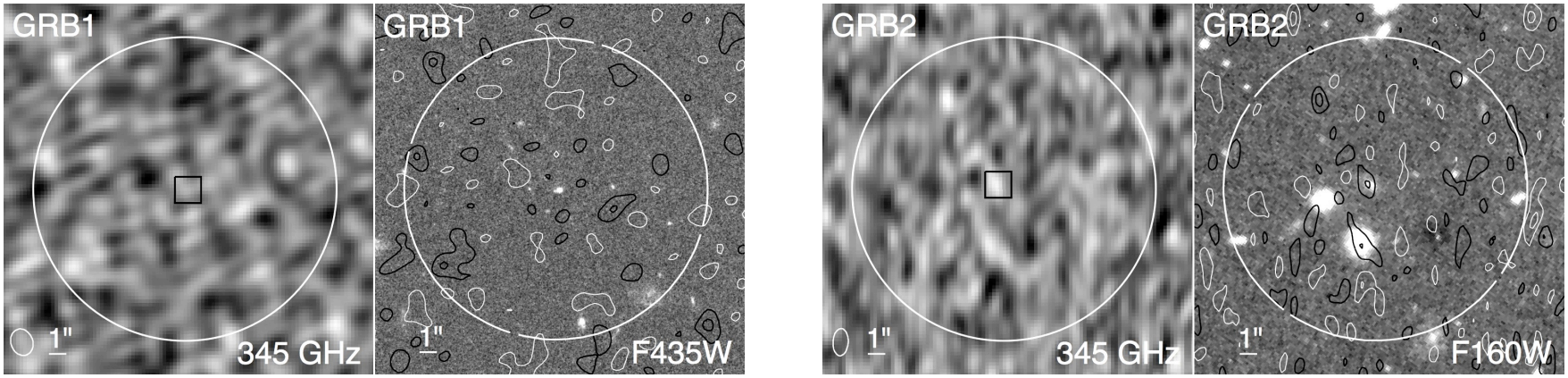

Wang, Chen, & Huang (2012, in prep)

- Both GRBs are optically faint (dark GRB), likely caused by dust extinction.
- ALMA reaches ~0.1 mJy (rms) sensitivity in <1 hr in each case.
  (It will take the SMA 81 nights to have a similar sensitivity.)
- GRB1 is not detected. $L_{IR} < 10^{11}\ L_\odot$, SFR < 20 $M_\odot$/yr.
- GRB2 is detected at 3.3 σ, with a flux of 0.313 ± 0.094 mJy.
  LIR ~ 2–4 × $10^{11}\ L_\odot$, SFR ~ 40–80 $M_\odot$/yr.
- Dark GRBs are probably normal disks, but not dusty ULIRGs.

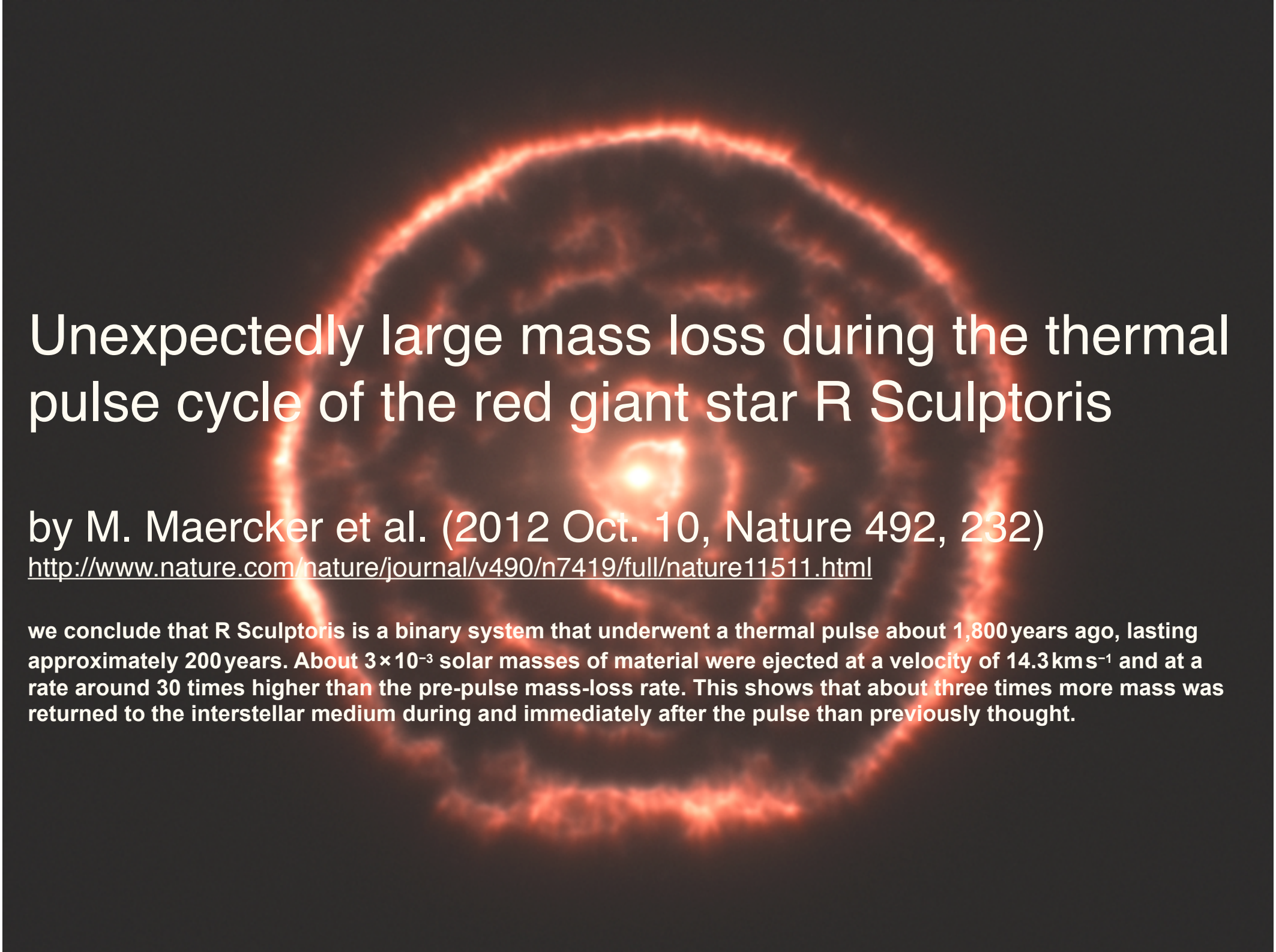

Unexpectedly large mass loss during the thermal pulse cycle of the red giant star R Sculptoris

by M. Maercker et al. (2012 Oct. 10, Nature 492, 232)
http://www.nature.com/nature/journal/v490/n7419/full/nature11511.html

we conclude that R Sculptoris is a binary system that underwent a thermal pulse about 1,800 years ago, lasting approximately 200 years. About 3×10^{-3} solar masses of material were ejected at a velocity of 14.3 km s^{-1} and at a rate around 30 times higher than the pre-pulse mass-loss rate. This shows that about three times more mass was returned to the interstellar medium during and immediately after the pulse than previously thought.

- Detached shells around (carbon-)stars - related to enhanced mass loss due to thermal pulses (helium flash)
  - an increase of expansion velocity is required to form shells

- ALMA Cycle 0
  - Band 3: CO (1-0), CN (1-0)
  - Band 6: CO (2-1), SiO (5-4)
  - Band 7: CO (3-2); 13CO(3-2), H13CN(3-2), CS(7-6)
  - Presented in this paper : Band 7 CO(3-2); compact config. with 6-hr observations; 45-point mosaic covering 50″x50″; 1.3″x1.0″ in resolution; r.m.s. ~ 44 mJy/beam per 0.5 km/s channel

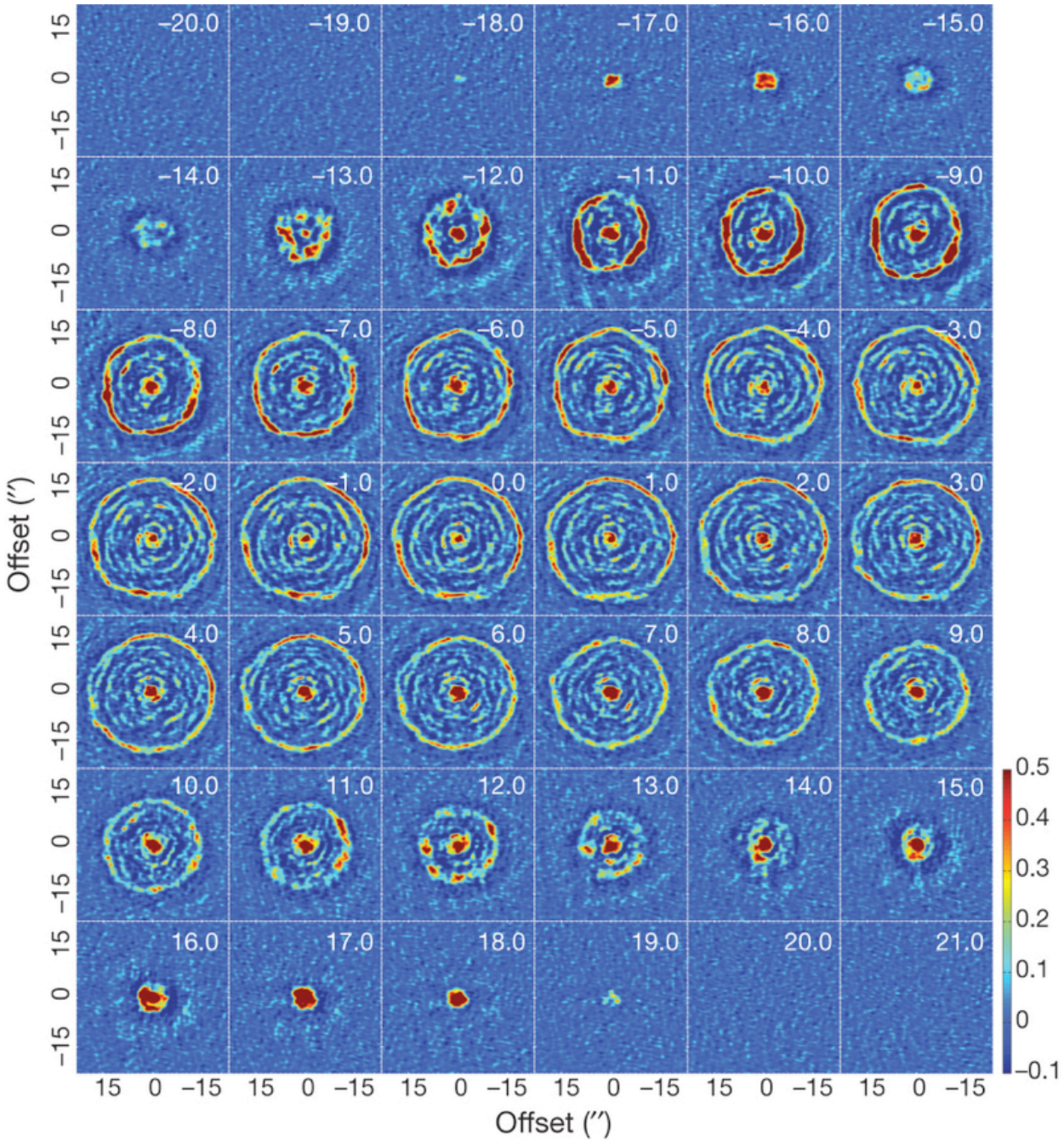

- **ALMA Early Science observations of the CO(J = 3−2) emission from the asymptotic-giant-branch star R Sculptoris.**

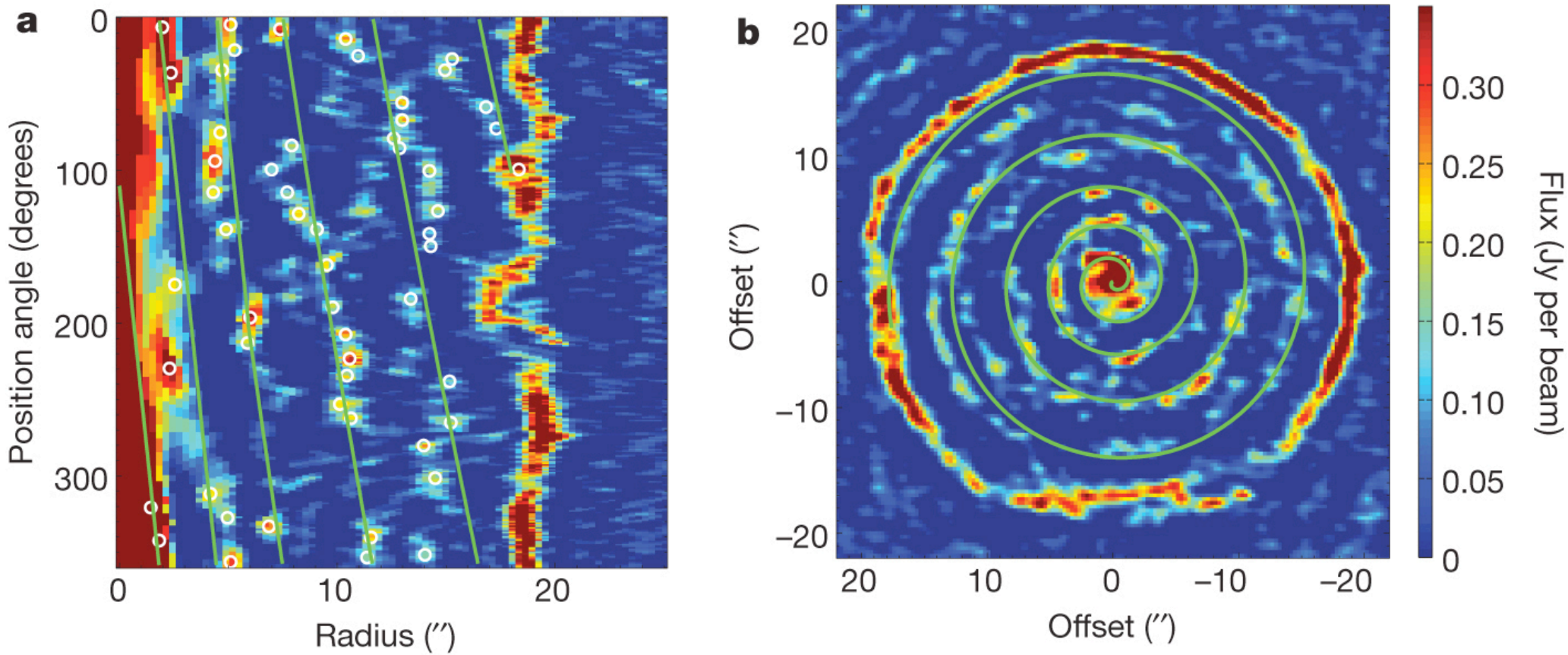

- **The CO(J = 3−2) emission at the stellar v_{LSR} of R Sculptoris.**

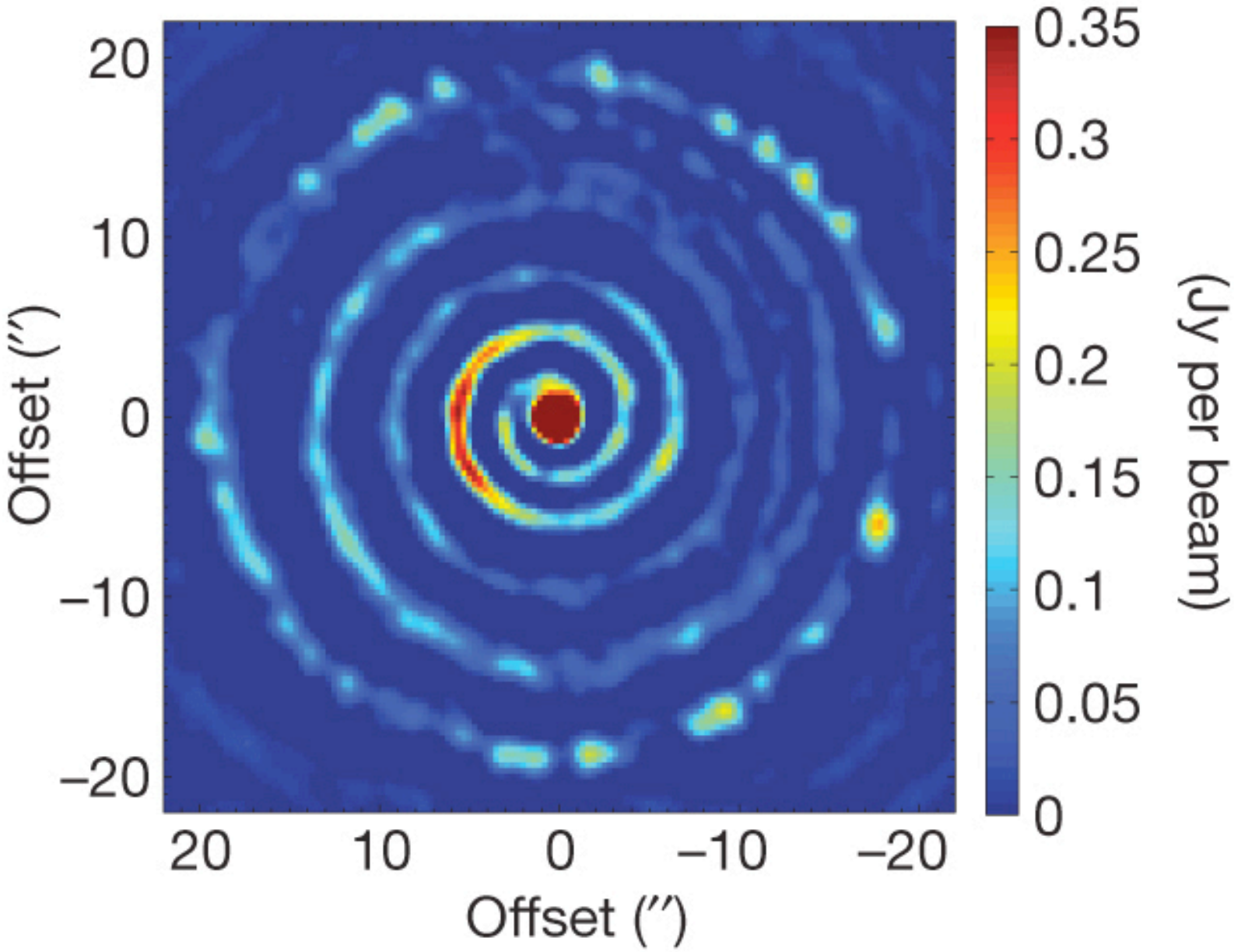

- **LIME radiative transfer model of the circumstellar structure around RSculptoris.**
  - **(GADGET 2) SPH -> LIME -> CASA**
  - **see movie at http://www.nature.com/nature/journal/v490/n7419/fig_tab/nature11511_SV1.html**

SMA Observations of Au Mic

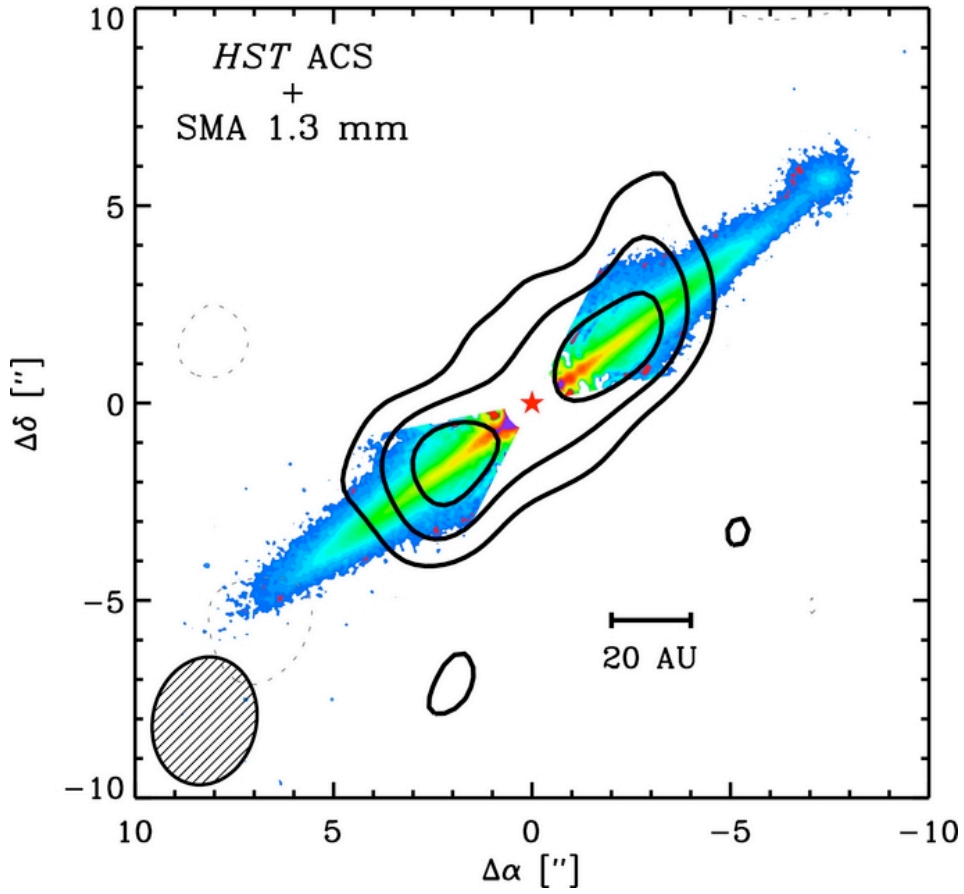

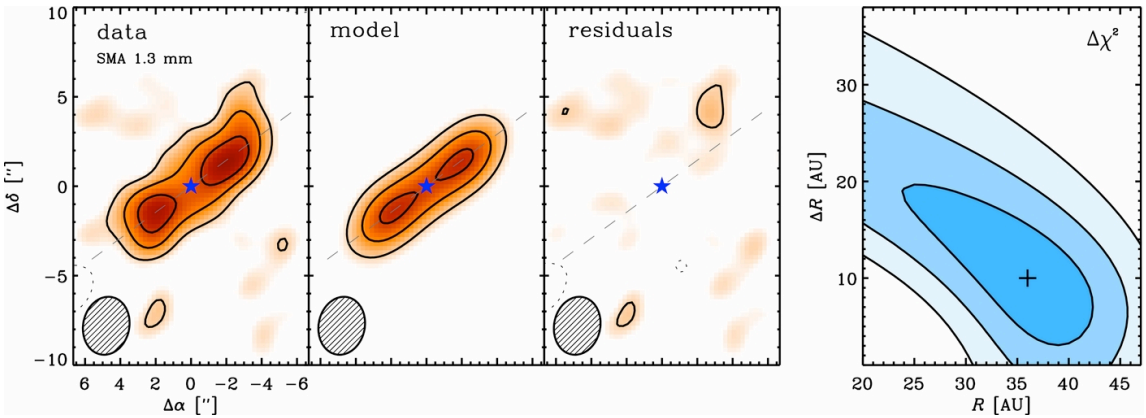

ALMA (B6) Cycle 0 data on Au Mic

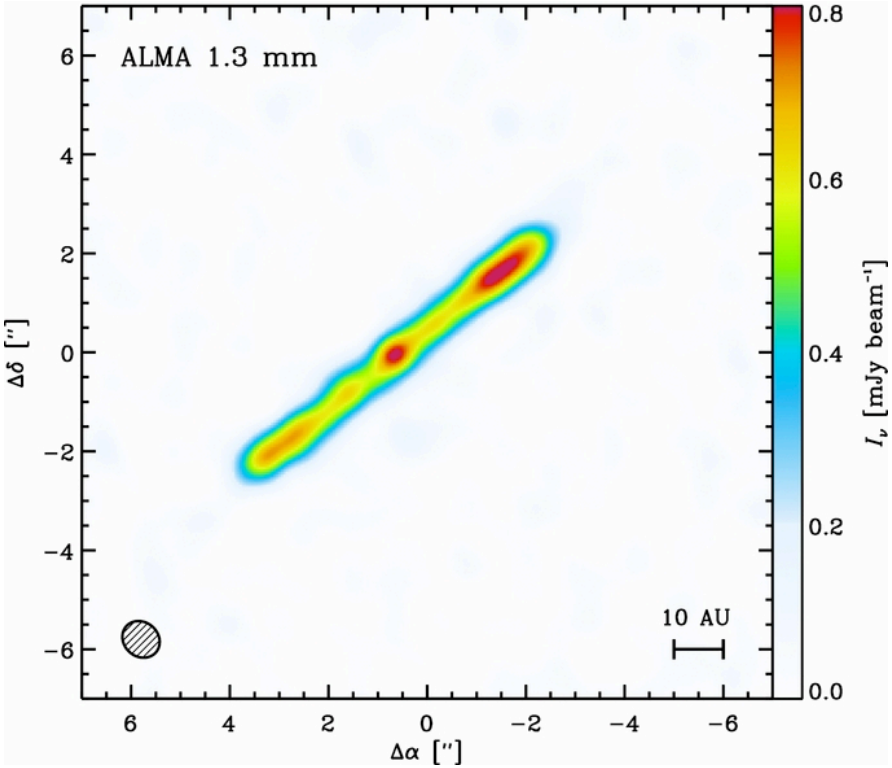

- The previously known dust belt that extends to a radius of 40 AU
- A newly recognized central peak that remains unresolved. dust emission from an inner planetesimal belt of mass ~0.01 M_{Moon}

Table 2
Model Parameters

Parameter	Description	Best-Fit	68% Confidence Interval
F_{belt}	Belt flux density (mJy)	7.14	+0.12, −0.25
x	Belt radial power law index	2.32	+0.21, −0.31
r_i	Belt inner radius (AU)	8.8	+11.0, −1.0
r_o	Belt outer radius (AU)	40.3	+0.4, −0.4
P.A.	Belt position angle (°)	128.41	+0.12, −0.13
α_{belt}	Belt spectral index	−0.15	+0.40, −0.58
F_{cen}	Gaussian flux density (mJy)	0.32	+0.06, −0.06
Δr_{cen}	Gaussian offset (AU)	0.71	+0.35, −0.51
σ^2_{cen}	Gaussian variance (AU^2)	$\leqslant$5.9	(3σ limit)
α_{cen}	Gaussian spectral index	−0.35	+2.1, −4.5
$\Delta\alpha$	R.A. offset of belt center (″)	0.61	+0.02, −0.02
$\Delta\delta$	Decl. offset of belt center (″)	−0.03	+0.02, −0.02

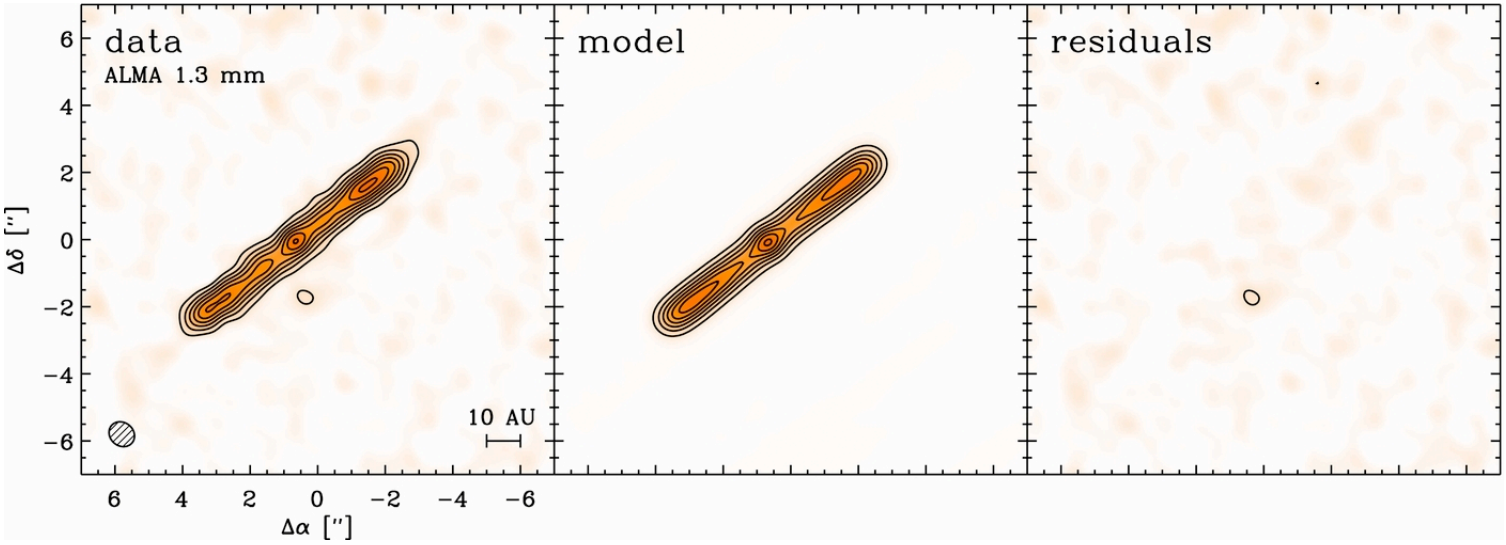

Final Remark

- most papers so far utilize SV data
- more papers are coming out with cycle 0 data
- lots of information and science are still possible with SV and cycle 0 data
- needs to work fast, though